Myelin oligodendrocyte glycoprotein–specific T and B cells cooperate to induce a Devic-like disease in mice

Estelle Bettelli,[1] Dominique Baeten,[2] Anneli Jäger,[1] Raymond A. Sobel,[3,4] and Vijay K. Kuchroo[1]

[1]Center for Neurologic Diseases, Brigham and Women's Hospital, Harvard Medical School, Boston, Massachusetts, USA.
[2]Division of Clinical Immunology and Rheumatology, Academic Medical Center, University of Amsterdam, Amsterdam, The Netherlands.
[3]Palo Alto VA Health Care System, Palo Alto, California, USA. [4]Department of Pathology, Stanford University School of Medicine, Stanford, California, USA.

Multiple sclerosis (MS) is a clinically and pathologically heterogeneous inflammatory/demyelinating disease of the CNS. In the MS variant Devic disease, lesions are predominantly found in the optic nerves and spinal cord but not the brain. The immunological bases of the different forms of MS are unknown. We previously generated myelin oligodendrocyte glycoprotein–specific (MOG-specific) TCR transgenic mice (TCR^MOG mice; also referred to as 2D2 mice) and reported that a large proportion of these mice develop spontaneous isolated optic neuritis. We have now crossed the TCR^MOG mice with MOG-specific Ig heavy-chain knock-in mice (IgH^MOG mice; also referred to as Th mice), in which one-third of the B cells are specific for MOG. In these mice, MOG-specific B cells are very efficient in presenting MOG to the transgenic T cells and undergo class switching to IgG1 in the presence of the transgenic T cells. Sixty percent of TCR^MOG×IgH^MOG mice spontaneously developed a severe form of experimental autoimmune encephalomyelitis (EAE). Histological examination of the CNS revealed a selective distribution of meningeal and parenchymal inflammatory lesions in the spinal cord and optic nerves. Thus, CNS antigen–specific T and B cells cooperate to induce a distinct clinicopathologic EAE pattern that closely replicates human Devic disease.

Introduction

MS is a clinically and pathologically heterogeneous disease most often characterized by inflammatory and demyelinating lesions throughout the CNS. There are several subtypes of the disease that differ in their CNS lesion distribution (1). Many MS patients first develop isolated optic neuritis, in which lesions are predominantly present in the optic nerves (2, 3). In Asian populations, Devic disease, or neuromyelitis optica (NMO), is the predominant subtype, representing one-third of MS cases (4). Patients with NMO often have a poor prognosis compared with patients with typical MS and develop severe and early relapses (5, 6). Devic disease is characterized by a specific lesion distribution in which inflammatory foci are restricted to optic nerves and the spinal cord with a remarkable absence of lesions in the brain (7). Antibodies (e.g., IgG and IgM) and products of the complement activation cascade have been found in and around CNS lesions, but a pathogenic role for autoantibodies in this disease subtype remains to be formally demonstrated (8). Interestingly, plasmapheresis has been reported to improve the neurologic outcome in patients with severe NMO (9), thereby supporting a role for humoral factors (possibly antibodies) in its pathogenesis.

The cellular and molecular bases for the different subtypes of MS are not well understood, but many features of the human disease have been recapitulated in the EAE animal model. EAE can be induced by immunization of susceptible animals with myelin antigens such as myelin basic protein (MBP), proteolipid protein (PLP), and myelin oligodendrocyte glycoprotein (MOG) (10–12); it is characterized by lymphocytic and mononuclear cell inflammatory infiltrates and demyelination in the brains and spinal cords of affected animals. Clinical manifestations of the disease depend on the antigen and the genetic background of the animal used. Immunization of SJL mice with the PLP aa 139–151 peptide, for example, induces episodes of relapsing-remitting disease in which the mice have a paralytic attack followed by periods of remission (11). On the other hand, immunization of C57BL/6 mice with MOG aa 33–55 produce a chronic form of EAE in which the animals stay paralyzed after their initial attack (12). Therefore each EAE model recapitulates some aspects of the human disease and provides valuable insight into the heterogeneous manifestations of MS.
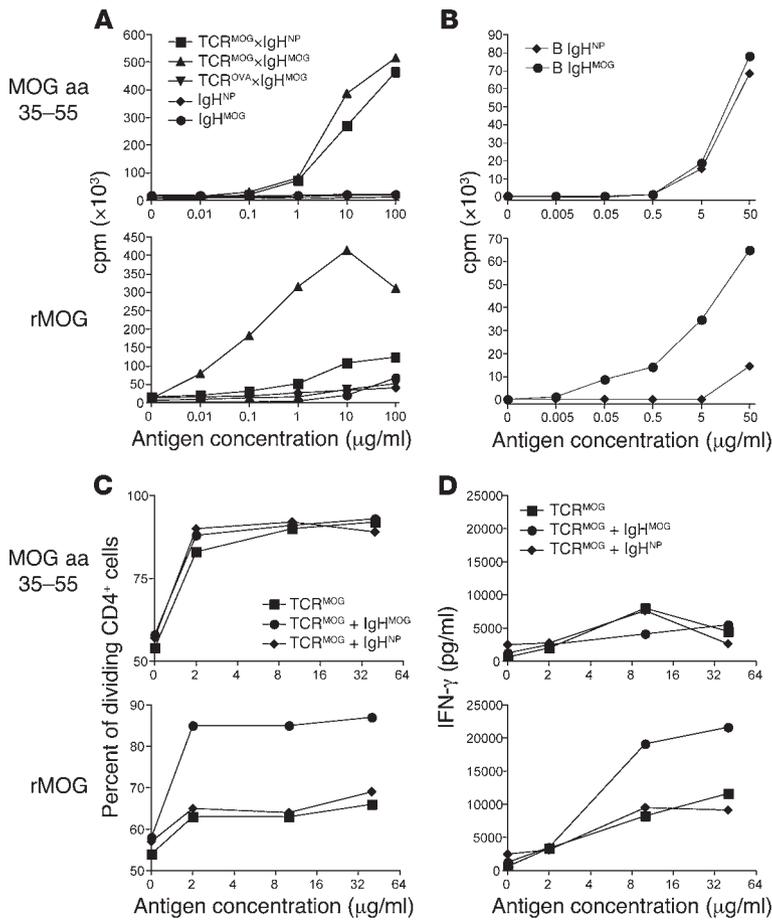
EAE can be induced by myelin antigen–specific Th1 cells (13, 14); more recently it has been suggested that Th-17 cells are major inducers of EAE (15, 16). By contrast, initial studies with immunization of B cell–deficient mice with the encephalitogenic peptide MOG aa 35–55 suggested that B cells may not be essential for the development of certain forms of EAE (17, 18). However, studies of immunization of B cell–deficient mice with recombinant whole MOG indicated a pathogenic role for B cells in the initiation of EAE (19–21), and other reports suggested that myelin antigen–specific B cells may act as regulatory cells and control the development of EAE (22). Therefore, the role of myelin antigen–specific B cells and antibodies in the pathogenesis of EAE as well as of MS are not well understood.

The result of interactions between myelin antigen–specific B cells and myelin antigen–specific T cells on the development and the phenotype of EAE have not previously been investigated. Here

Figure 1
MOG-specific B cells enhance antigen presentation to MOG-specific T cells. (**A**) Proliferation of splenocytes from TCR^{MOG}×IgH^{MOG}, TCR^{MOG}×IgH^{NP}, IgH^{MOG}, IgH^{NP}, and TCR^{OVA}×IgH^{MOG} mice incubated with different doses of MOG aa 35–55 peptide or rMOG protein as antigen. (**B**) Proliferation of TCR^{MOG} T cells cultured in the presence of purified MOG (IgH^{MOG}) or NP-specific (IgH^{NP}) B cells and increasing doses of antigen. (**C** and **D**) Splenocytes from TCR^{MOG} mice were stimulated in vitro with increasing doses of MOG aa 35–55 peptide or rMOG protein, either alone or in the presence of MOG-specific B lymphocytes (IgH^{MOG}) or NP-specific B lymphocytes (IgH^{NP}) as control. (**C**) Proliferation of MOG-specific T lymphocytes was measured by CFSE labeling of CD4$^+$ T cells after 3 days of culture. (**D**) Cytokine secretion in the culture supernatants was measured by ELISA after 4 days of culture. Data are representative of at least 3 independent experiments.

we hypothesized that MOG-specific B cells could activate TCR^{MOG} T cells and induce spontaneous EAE in the TCR^{MOG} mice. Therefore, we crossed the TCR^{MOG} mice with MOG-specific Ig heavy-chain knock-in mice on a C57BL/6 background (IgH^{MOG} mice; also referred to as Th mice), in which 20% of peripheral B cells are specific for the autoantigen MOG (24), thus providing B and T cells specific for the same MOG antigen in the peripheral repertoire of the mice.

To determine whether the presence of MOG-specific B cells could change the T cell response of TCR^{MOG} T cells in TCR^{MOG}×IgH^{MOG} mice, we first analyzed the proliferation of splenocytes from TCR^{MOG}×IgH^{MOG} and control TCR^{MOG} mice crossed with nitrophenyl-specific (NP-specific) Ig heavy-chain knock-in mice on a C57BL/6 background (TCR^{MOG}×IgH^{NP} mice; IgH^{NP} also referred to as B1.8 mice) in response to MOG aa 35–55 peptide or whole recombinant MOG aa 1–125 (rMOG) protein. Splenocytes from TCR^{MOG}×IgH^{MOG} mice, carrying MOG-specific T and B cells, and TCR^{MOG}×IgH^{NP} mice, carrying MOG-specific T cells and NP-specific B cells, proliferated equally well in response to MOG aa 35–55 peptide (Figure 1A). As a control, splenocytes from IgH^{MOG} mice, IgH^{NP} mice, and OVA-specific TCR transgenic mice on a C57BL/6 background (TCR^{OVA} mice; also referred to as OT-II mice) crossed with IgH^{MOG} mice (TCR^{OVA}×IgH^{MOG} mice), all lacking the MOG-specific T cells, did not respond to MOG aa 35–55 peptide (Figure 1A). Similarly, splenocytes from IgH^{NP}, IgH^{MOG}, or TCR^{OVA}×IgH^{MOG} mice did not proliferate in response to whole rMOG (Figure 1A). However, splenocytes from TCR^{MOG}×IgH^{MOG} mice, which express MOG-specific T and B cells, proliferated more strongly and at lower concentrations to rMOG than the control TCR^{MOG}×IgH^{NP} mice (Figure 1A).

MOG-specific B cells enhance antigen presentation to MOG-specific T cells. The enhanced response of TCR^{MOG}×IgH^{MOG} splenocytes to rMOG could be attributed to the proliferation of either T or B cells or both. To determine which cell type was responsible for the enhanced proliferation, we first tested the response of T cells in the presence of B cells of different specificities. We initially separated T cells from the spleens of TCR^{MOG} mice and stimulated them with purified B cells from either IgH^{NP} or IgH^{MOG} mice together with MOG aa 35–55 peptide or rMOG protein as a source of specific antigen. Whereas MOG aa 35–55 peptide

we describe a mouse EAE model in which both T and B cells are specific for the same autoantigen MOG. The presence of MOG-specific B and T cells in the peripheral repertoire resulted in the development of severe and spontaneous EAE in the majority of the mice. Histopathological analysis of the CNS of the affected mice showed a preponderance of inflammatory lesions in the leptomeninges and parenchyma of the spinal cords and optic nerves but not in the brains of affected mice. Our results suggest that an active cooperation between MOG-specific T and B cells results in a spontaneous and severe form of EAE with a lesion distribution pattern typical of human Devic disease.
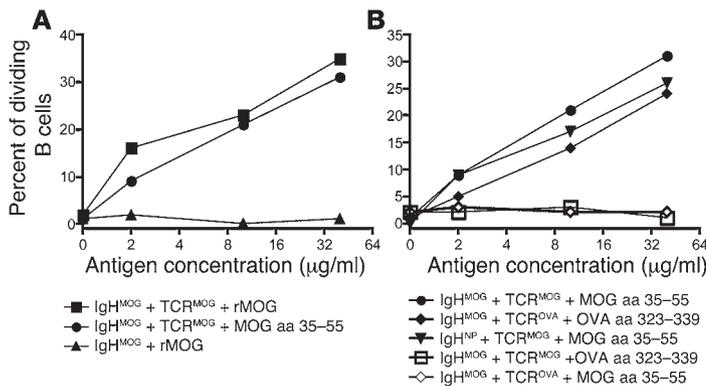
Results

Enhanced MOG-specific splenocyte proliferation in TCR^{MOG}×IgH^{MOG} mice. We previously generated MOG-specific TCR transgenic mice on a C57BL/6 background (TCR^{MOG} mice; also referred to as 2D2 mice) in which the transgenic TCR-bearing cells are efficiently selected in the thymus and are seeded to the peripheral immune compartment (23). Although over 95% of the peripheral T cells express transgenic TCR, only a small percentage (4%) of TCR^{MOG} mice develop spontaneous EAE. Nevertheless, a significant number of the transgenic mice develop spontaneous optic neuritis (47%). Immunization of TCR^{MOG} mice with the MOG peptide in complete Freund's adjuvant plus pertussis toxin resulted in the development of full-blown EAE, suggesting that EAE can be induced in the transgenic mice if there is appropriate activation of transgenic TCR^{MOG} T cells. Since antigen-specific B cells can be efficient APCs,

Figure 2
Proliferation of MOG-specific B lymphocytes upon stimulation with activated T lymphocytes. (**A**) IgH^{MOG} B lymphocytes were cultured in the presence of T cells from TCR^{MOG} mice. (**B**) IgH^{MOG} and IgH^{NP} B lymphocytes were cultured in the presence of T cells from TCR^{MOG} or TCR^{OVA} mice. Cultures were stimulated with increasing doses (0–40 μg/ml) of rMOG protein, MOG aa 35–55 peptide, or OVA aa 323–339 peptide as indicated. Proliferation of B lymphocytes was measured by CFSE labeling of B220$^+$ cells after 4 days of culture.

induced a strong proliferation of MOG-specific T cells independently of the presence of specific B cell populations, whole rMOG protein led only to dose-dependent proliferation in the presence of MOG-specific B lymphocytes (Figure 1B). To confirm that the observed response corresponded to T cell proliferation, we stimulated CFSE-labeled splenocytes of TCR^{MOG} mice in the presence of MOG-specific B cells (IgH^{MOG}) or NP-specific B cells (IgH^{NP}) and different concentrations of MOG aa 35–55 peptide or rMOG and measured T cell proliferation by CFSE dilution on CD4$^+$ T cells. Using this approach we observed similar numbers of dividing TCR^{MOG} T cells in response to MOG aa 35–55 peptide independent of the antigen specificity of the B cells used as APCs (Figure 1C). In contrast, more TCR^{MOG} T cells divided in response to rMOG in the presence of IgH^{MOG} MOG-specific B cells than in the presence of IgH^{NP} NP-specific B cells, confirming that provision of MOG-specific B cells to T cells of the same specificity enhanced their proliferative response (Figure 1C and Supplemental Figure 1; supplemental material available online with this article; doi:10.1172/JCI28334DS1).

Next we analyzed T cell cytokines secreted under these culture conditions. Stimulation of TCR^{MOG} T cells with rMOG and B cells led to a dose-dependent secretion of IFN-γ. IFN-γ production in response to rMOG was greater in the presence of MOG-specific IgH^{MOG} B cells than in the presence of NP-specific B cells (Figure 1D). Intracellular anti–IFN-γ staining of CD4$^+$ T cells confirmed that MOG-specific CD4$^+$ T cells were responsible for the increased IFN-γ production observed (data not shown). In contrast, IFN-γ levels were comparable among T cells stimulated with MOG aa 35–55 peptide, IgH^{MOG} B cells, and IgH^{NP} B cells (Figure 1D). These data

suggest that the MOG protein is selectively processed (25) and presented by MOG-specific B cells, resulting in more efficient activation of MOG-specific T cells when both cell types are present in the peripheral repertoire. The Th2-associated cytokines IL-4 and IL-10 and the pathogenic cytokine IL-17, which is the signature of Th-17 cells, could not be detected in the supernatants (data not shown).

Activated T cells are essential for proliferation of IgH^{MOG} B cells. Next we analyzed the role of B cells in the enhanced response of TCR^{MOG}×IgH^{MOG} splenocytes to rMOG. B cells were purified from either IgH^{MOG} (MOG-specific) mice or IgH^{NP} (NP-specific) mice, labeled with CFSE, and cultured in the presence of purified T cells from either TCR^{MOG} (MOG aa 35–55–specific) mice or TCR^{OVA} (OVA aa 323–339–specific) mice. B cell proliferation was evaluated by CFSE dilution on B220$^+$ B cells, and different cell surface activation molecules were assessed by flow cytometry analysis. Provision of MOG protein to MOG-specific B cells was not sufficient to trigger B cell division (Figure 2A). Coculture with activated TCR^{MOG} T cell lines and MOG led to a dose-dependent proliferation of MOG-specific IgH^{MOG} B lymphocytes (Figure 2A) and upregulation of activation markers such as CD69, CD80, and CD86 (Supplemental Figure 2 and data not shown). However, MOG-specific B cells also proliferated upon coculture with activated OVA-specific T cell lines and rMOG, as did NP-specific B cells upon coculture with activated MOG-specific T cells (Figure 2B). These results show that, in vitro, the presence of activated T cells alone rather than antigen-specific T cells is sufficient for the induction of B lymphocyte proliferation.

Mice carrying MOG-specific T and B cells develop severe EAE. We previously reported that very few (4%) TCR^{MOG} mice develop spontaneous EAE, but a significant portion develops isolated optic neuritis

Table 1

Spontaneous Devic-like disease in TCR^{MOG}×IgH^{MOG} mice

Mouse	Specificity		Clinical disease			Histological disease	
	T cells	B cells	Incidence	Mean clinical score	Age of onset (d)	No. inflammatory foci	Incidence of Devic-like disease[A]
TCR^{MOG}	MOG	-	5/81 (6%)	1.4 ± 0.4	73.5 ± 7.7	16.6 ± 11.2	0/3
IgH^{MOG}	-	MOG	0/70 (0%)	NA	NA	0 ± 0	0/6
TCR^{MOG}×IgH^{MOG}	MOG	MOG	29/49 (59%)	2.9 ± 0.05	44.1 ± 2.8	188.4 ± 48.3	10/10
IgH^{NP}	-	NP	0/20 (0%)	NA	NA	0 ± 0	0/5
TCR^{MOG}×IgH^{NP}	MOG	NP	0/27 (0%)	NA	NA	0.25 ± 0.25	0/4
TCR^{OVA}×IgH^{MOG}	OVA	MOG	0/17 (0%)	NA	NA	ND	ND

Mice were observed for a period of 3 months for the development of spontaneous clinical signs of EAE. [A]Devic-like disease was defined by inflammatory foci specifically localized in the spinal cord and optic nerves. ND, not determined.

Table 2
Distribution of parenchymal inflammatory lesions in the CNS of TCR^{MOG}×IgH^{MOG} and TCR^{MOG} mice

Mouse	Cerebral hemispheres (% ± SE)	Midbrain brainstem (% ± SE)	Cerebellum (% ± SE)	Spinal cord (% ± SE)	Total parenchymal inflammatory foci (± SE)	Incidence of optic neuritis[A]
TCR^{MOG}×IgH^{MOG}	2.1 ± 0.9	3.2 ± 1.9	3.3 ± 2.3	91.4 ± 4.4	90.6 ± 5.0	10/10
TCR^{MOG}	40 ± 7	18 ± 6	24 ± 11	18 ± 13	45 ± 25	2/2

CNS parenchymal lesion distribution in TCR^{MOG}×IgH^{MOG} mice with spontaneous Devic-like disease ($n = 10$) and TCR^{MOG} mice with spontaneous EAE ($n = 2$) are compared. The number of parenchymal inflammatory lesions was counted in the different anatomic regions of the CNS and are expressed as mean percent of total parenchymal foci ± SE in the group. The mean total inflammatory parenchymal lesions ± SE and the incidence of optic neuritis are indicated. [A]All mice analyzed had optic neuritis.

(23). We also found that the development of full-blown EAE in TCR^{MOG} mice was in part dependent on the immunization regimen, suggesting that isolated optic neuritis may progress to EAE if there is appropriate activation of MOG-specific T cells. Based on our in vitro data indicating that antigen-specific B cells efficiently activated MOG-specific T cells, we followed the development of spontaneous EAE in TCR^{MOG}×IgH^{MOG} and control mice.
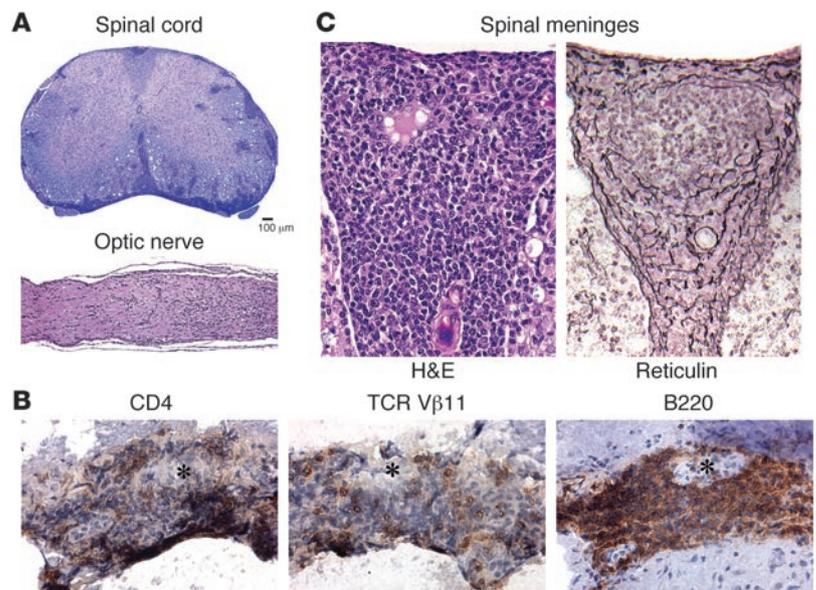
Consistent with previous reports, no spontaneous EAE was observed in IgH^{MOG} mice (24), and TCR^{MOG} mice developed a very low incidence of spontaneous EAE (6%; Table 1). The presence of transgenic T cells of a different specificity (OVA specific) also did not result in the development of spontaneous EAE in TCR^{OVA}×IgH^{MOG} mice (Table 1). In sharp contrast, 59% of TCR^{MOG}×IgH^{MOG} mice carrying MOG-specific T and B cells developed severe EAE (Table 1). The disease had an abrupt onset with rapid progression to a clinical score of 2.5–3 over 1–2 days in most mice with disease (Supplemental Figure 3). We did not observe any gender bias for the development of spontaneous disease in TCR^{MOG}×IgH^{MOG} mice. Incidence as well as mean clinical scores among TCR^{MOG}×IgH^{MOG} mice were higher than in TCR^{MOG} mice with spontaneous EAE. Spontaneous disease was also accelerated in that it developed earlier in TCR^{MOG}×IgH^{MOG} mice (44.1 days after birth) than in TCR^{MOG} mice (73.5 days after birth). Mortality among TCR^{MOG}×IgH^{MOG} mice was 10% (3 of 29), compared with 0% (0 of 5) in TCR^{MOG} mice. The severity of the disease was also apparent histologically, as TCR^{MOG}×IgH^{MOG} mice

had a mean of 188.4 CNS inflammatory foci compared with 16.6 in the TCR^{MOG} mice (Table 1). No histologic disease was observed in TCR^{MOG}×IgH^{MOG} mice without clinical disease, TCR^{MOG}×IgH^{NP} mice, or IgH^{MOG} mice (Table 1). These results suggested that the presence of MOG-specific B cells is crucial for increased incidence and severity of spontaneous EAE in TCR^{MOG} mice.

Distinct lesion localization in TCR^{MOG}×IgH^{MOG} mice. We determined the anatomic localization of inflammatory lesions in the different areas of the CNS of TCR^{MOG} and TCR^{MOG}×IgH^{MOG} with EAE. In TCR^{MOG} mice with EAE, most of the lesions (40%) were localized in the cerebral hemispheres (Table 2). The remaining foci were equally distributed among the midbrain-brainstem, the cerebellum, and the spinal cord. These mice also had optic neuritis. In contrast, most of the lesions of TCR^{MOG}×IgH^{MOG} mice were localized in their spinal cords and optic nerves, with very few in the brain (less than 3% in cerebral hemispheres, midbrain-brainstem, or cerebellum; Table 2 and Figure 3A). This lesion distribution pattern is similar to that of Devic disease. This selective distribution of inflammatory foci in the spinal cords and optic nerves was observed in 100% of the affected TCR^{MOG}×IgH^{MOG} mice analyzed histologically (Table 1), but not in TCR^{MOG} mice with EAE. The inflammatory lesions were composed of lymphocytes and monocytes and were present in both leptomeninges and parenchyma, particularly the subpial regions where there was marked associated demyelination and edema (Figure 3A). Peripheral nerve

Figure 3
Histopathological analysis of CNS tissues of TCR^{MOG}×IgH^{MOG} mice with Devic-like disease. (**A**) Paraffin sections show extensive mononuclear cell infiltrates in meninges and spinal cord (upper panel, Luxol fast blue–H&E stain; original magnification, ×16) and optic neuritis (lower panel, H&E stain; original magnification, ×40) of TCR^{MOG}×IgH^{MOG} mice. (**B**) Cryosections of TCR^{MOG}×IgH^{MOG} spinal cord showing T cell (anti-CD4 and anti-Vβ11 staining) and prominent B cell infiltrates in the subarachnoid space. Asterisks indicate the same vessel in each section. Original magnification, ×160. (**C**) Paraffin sections showing a spinal cord leptomeningeal infiltrate composed primarily of lymphocytes (H&E stain). The adjacent section shows a follicle-like organization pattern (reticulin stain). Original magnification, ×160.

A

TCR^MOG   **TCR^MOG×IgH^MOG, healthy**   **TCR^MOG×IgH^MOG, sick**

1.8   2.4   4.7 — Spleen

3.1   4.1   8.2 — Lymph nodes

CD69 / CD4

B

WT   IgH^MOG   TCR^MOG×IgH^MOG, healthy   TCR^MOG×IgH^MOG, sick

B7.1: 2.8   2.8   2.6   4.6

B7.2: 1.0   0.9   1.6   1.5

B220

C

IgM (OD); IgG1 (OD); IgG2a (OD); IgG2b (OD)

Figure 4

Phenotypic analysis of T and B cells and MOG-specific antibodies in TCR^MOG×IgH^MOG mice. (**A**) Surface staining of CD69 on CD4+ T cells in the spleens and lymph nodes of TCR^MOG mice as well as healthy and sick TCR^MOG×IgH^MOG mice. The percentage of CD69+ cells in CD4+ T cells is indicated. (**B**) Expression of B7.1 and B7.2 on splenic B cells (B220+) from WT and IgH^MOG mice as well as healthy and sick TCR^MOG×IgH^MOG mice. The percentage of B220+B7.1+ or B220+B7.2+ cells is indicated. Dot plots in **A** and **B** are representative of 3 experiments. (**C**) MOG-specific antibodies in serum samples from individual mice were measured by ELISA for the different isotypes: IgM, IgG1, IgG2a, IgG2b, and IgG3. Isotype IgG3 was below the detection level in all groups (not shown). Results are expressed as OD; horizontal bars indicate mean OD for each group.

roots were intact. Phenotypic analysis on cryosections demonstrated infiltration of T cells (CD4+ and TCR Vβ11+) and large numbers of B cells (B220+; Figure 3B). The accumulations of lymphocytes were particularly marked in the subarachnoid spaces around the spinal cord of TCR^MOG×IgH^MOG mice, and the aggregates focally formed follicle-like structures that were made evident using reticulin stains (Figure 3C). Similar patterns of germinal center–like structures have previously been described in the leptomeninges of patients with MS (26, 27). We did not identify substantial numbers of eosinophils or neutrophils in these lesions. Collectively, these data indicate that TCR^MOG×IgH^MOG mice have a selective Devic-like distribution of inflammatory lesions, i.e., in the spinal cord and the optic nerves, which is characterized by a close and well-organized follicle-like architecture that may allow close interaction between antigen-specific T and B cell populations in the target tissue.

Ex vivo analysis of MOG-specific T and B cells and circulating antibodies. To obtain insight into the mechanisms responsible for the development of Devic-like disease in TCR^MOG×IgH^MOG mice, we analyzed the phenotype of both T and B cells ex vivo. Between 6 and 8 weeks of age, CD4+ T cells from TCR^MOG mice were mostly naive, and only 1.8% of them were activated/memory cells
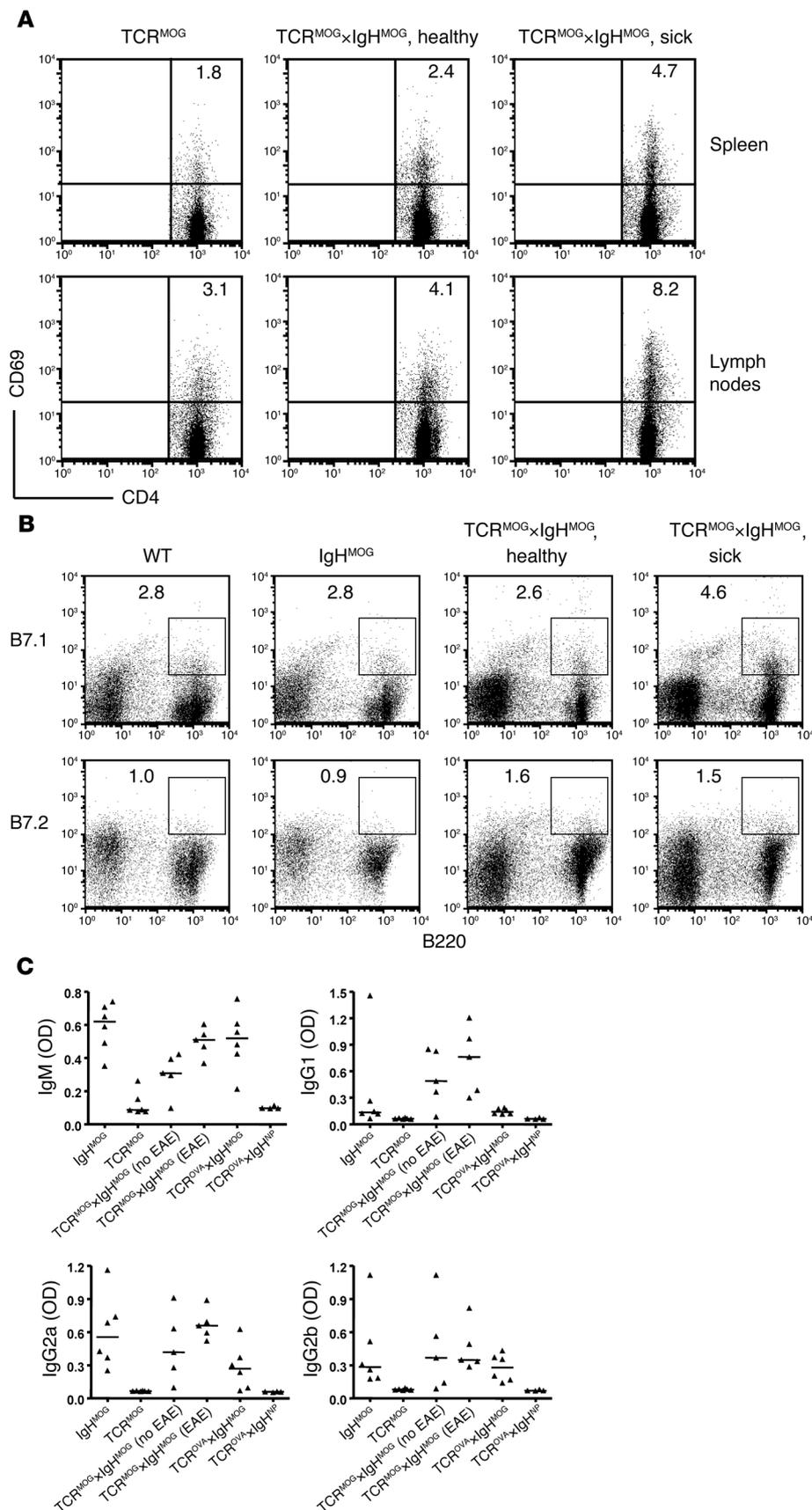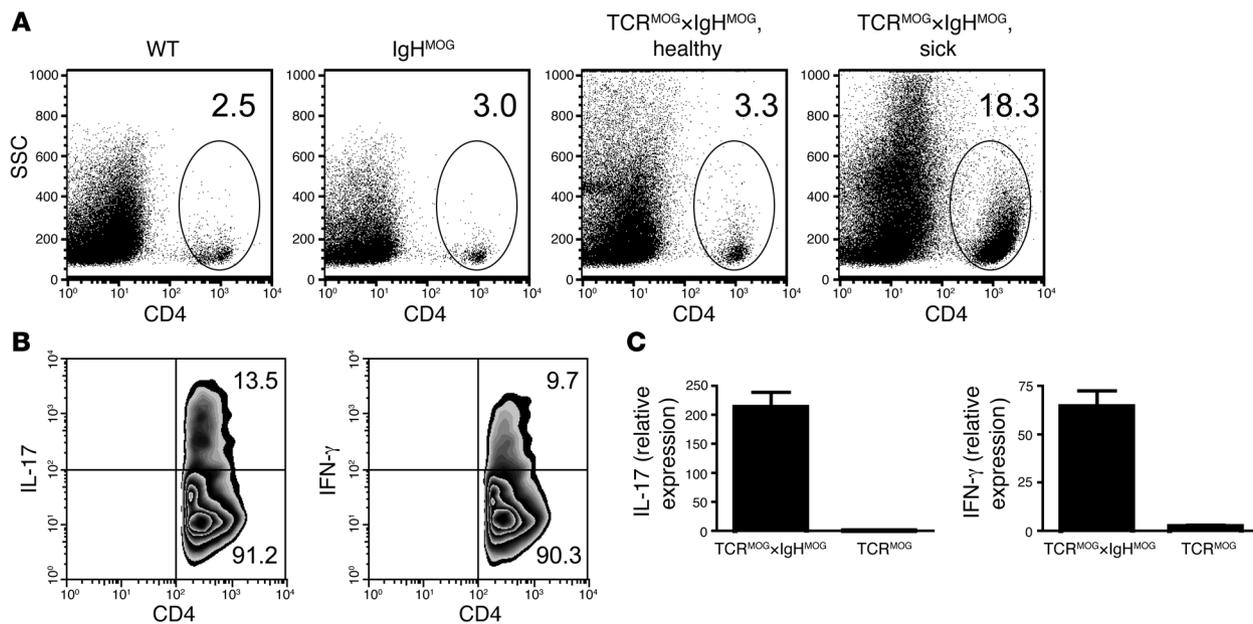
Figure 5
IL-17– and IFN-γ–producing CD4+ T cells infiltrate the CNS of TCR^{MOG}×IgH^{MOG} mice with Devic disease. (**A**) Mononuclear cells from the brains and spinal cords of WT and IgH^{MOG} mice as well as healthy and sick TCR^{MOG}×IgH^{MOG} mice were isolated by percoll gradient and stained with anti-CD4 antibody. Dot plots show CD4 expression versus side scatter (SSC). The percentage of CD4+ T cells present in the gate is indicated. (**B**) Mononuclear cells isolated from the brains and spinal cords of TCR^{MOG}×IgH^{MOG} mice with Devic disease were stimulated with PMA and ionomycin, and the presence of IL-17– and IFN-γ–secreting CD4+ T cells was determined by intracellular cytokine staining. The percentage of IL-17– and IFN-γ–positive and –negative cells in CD4+ T cells is indicated in each dot plot. (**C**) RNA was prepared from the spinal cords of TCR^{MOG} mice with EAE (n = 2) and TCR^{MOG}×IgH^{MOG} mice with Devic-like disease (n = 2). Expression of IL-17 and IFN-γ cDNAs was determined by real-time PCR, and results are expressed as relative to β-actin.

in the spleen (Figure 4A). Healthy TCR^{MOG}×IgH^{MOG} mice had similar numbers of activated cells (2.4%). In contrast, an increased proportion of CD4+ T cells (4.7% and 8.2% in spleens and lymph nodes, respectively) from diseased TCR^{MOG}×IgH^{MOG} mice were activated and expressed CD69 (Figure 4A). Analysis of the number of regulatory cells, as determined by Foxp3 intracellular staining in CD4+ T cells, showed a small but comparable number of CD4+Foxp3+ T cells (2%) in the spleens and lymph nodes of healthy and diseased TCR^{MOG}×IgH^{MOG} mice (data not shown).

Next we looked at the expression of different markers on the surface of B cells from the various mouse strains. We did not find any difference in the expression of MHC class II molecules, B7.2, or IgM^a on the surface of B cells from IgH^{MOG} or healthy or diseased TCR^{MOG}×IgH^{MOG} mice (Figure 4B and data not shown). However, we observed an increase in the percentage of B220+B7.1+ cells in the spleens of TCR^{MOG}×IgH^{MOG} mice with disease compared with healthy TCR^{MOG}×IgH^{MOG} mice. The upregulation of the B7.1 molecule on the surface of B cells in TCR^{MOG}×IgH^{MOG} mice with Devic-like disease suggests that these B cells have been activated. To determine whether MOG-specific B cells differentiated into effector B cells, we measured levels of MOG-specific antibodies in serum samples of IgH^{MOG}, TCR^{MOG}, TCR^{MOG}×IgH^{MOG}, TCR^{OVA}×IgH^{MOG}, and TCR^{MOG}×IgH^{NP} mice. No MOG-specific antibodies were detected in the absence of IgH^{MOG} MOG-specific B cells, i.e., in TCR^{MOG} mice and in TCR^{MOG}×IgH^{NP} mice. Without any immunization, IgH^{MOG} mice and TCR^{OVA}×IgH^{MOG} mice produced large amounts of MOG-specific IgM, IgG2a, and IgG2b antibodies but low levels of IgG1 (Figure 4C). In contrast, serum samples from TCR^{MOG}×IgH^{MOG} mice, in which

MOG-specific T cells and B cells are present in the peripheral repertoire, contained lower amounts of MOG-specific IgM (P = 0.04) but higher amounts of MOG-specific IgG1 antibodies (P = 0.03) than the IgH^{MOG} and TCR^{OVA}×IgH^{MOG} mice. MOG-specific antibody isotype switching to IgG1 was consistently found in all TCR^{MOG}×IgH^{MOG} mice analyzed, whether they had clinical EAE or were asymptomatic (Figure 4C). Isotype switching was not dependent on age, since serum samples obtained from 4-week-old and adult TCR^{MOG}×IgH^{MOG} mice showed high levels of anti-MOG IgG1 antibodies.

IL-17– and IFN-γ–secreting CD4+ T cells infiltrate the CNS of TCR^{MOG}×IgH^{MOG} mice with Devic-like disease. To further characterize the MOG-specific T cell responses involved in the development of Devic-like disease, we purified mononuclear cells from WT, IgH^{MOG}, and healthy and diseased TCR^{MOG}×IgH^{MOG} mice. Consistent with the absence of disease in the WT, IgH^{MOG}, and healthy TCR^{MOG}×IgH^{MOG} mice, there were small numbers of mononuclear cells present in the CNS of these animals (data not shown). In these 3 strains of mice, CD4+ T cells represented 3% of the few infiltrating monocytes. However, in TCR^{MOG}×IgH^{MOG} mice with Devic-like disease, there was an increase in the number of infiltrating monocytes (data not shown) and a 5-fold increase in the percentage of CD4+ T cells in the CNS tissues (Figure 5A). Since both Th1 and Th-17 cells have been implicated in the development of EAE (15, 16, 28, 29), we determined whether T cells from TCR^{MOG}×IgH^{MOG} mice with EAE could secrete these cytokines. Although IL-17 production was not detected in our in vitro cultures (data not shown), intracellular cytokine staining of CD4+ T cells obtained from the CNS of TCR^{MOG}×IgH^{MOG} mice showed that CD4+ T cells involved in
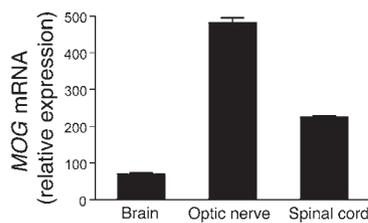
Figure 6
MOG mRNA is more abundant in the spinal cord than in the brain. Brains, spinal cords, and optic nerves were isolated from C57BL/6 mice (*n* = 18) and pooled to prepare mRNA. Expression of *MOG* mRNA was determined by real-time PCR and expressed as relative to β-actin.

the development of Devic-like disease secreted IFN-γ and IL-17 (Figure 5B). Since only 4% of TCR^MOG mice develop spontaneous EAE, it has not been possible to obtain CNS samples from these animals to perform FACS analysis together with those of TCR^MOG×IgH^MOG mice with disease. However, we have prepared RNA from the spinal cords of TCR^MOG×IgH^MOG mice with Devic-like disease and TCR^MOG mice with spontaneous EAE and analyzed the expression of *IL-17* mRNA by real-time PCR. This analysis showed that there was an increase in expression of both *IL-17* and *IFN-γ* mRNA in the spinal cords of diseased TCR^MOG×IgH^MOG mice compared with TCR^MOG mice with EAE (Figure 5C). Although we could not determine which cell type was responsible for the increased IL-17 and IFN-γ production observed in the spinal cords of TCR^MOG×IgH^MOG mice, together with the intracellular cytokine staining, these data suggest that more Th1 and Th-17 cells are infiltrating the spinal cords of TCR^MOG×IgH^MOG mice than do so in TCR^MOG mice.

MOG mRNA is more abundant in the spinal cord than in the brain. While the enhanced and selective activation of TCR^MOG T cells in the presence of MOG-specific B cells can explain the high incidence of spontaneous disease observed in TCR^MOG×IgH^MOG mice compared with TCR^MOG mice, it is not clear why TCR^MOG×IgH^MOG mice have Devic-like disease and not typical EAE. To begin to address this issue, we compared the expression of the autoantigen MOG in different CNS regions of C57BL/6 mice. Consistent with our previous observation (23), we found that *MOG* mRNA was more abundant in the optic nerve than the spinal cord (Figure 6). We also found that *MOG* mRNA was more abundant in the spinal cord than in the brain. This selective distribution of *MOG* mRNA might contribute at least in part to the preferential localization of lesions in the spinal cords and optic nerves of TCR^MOG×IgH^MOG mice.

Discussion

Here we report the generation of what we believe to be a new mouse model in which both T and B cells are specific for the same myelin antigen, MOG. We demonstrated that there was active cooperation between T and B cells in these animals: the presence of MOG-specific T cells led to massive production of MOG-specific IgG1 antibody, and MOG-specific B cells also enhanced MOG-specific T cell proliferation and activation. Strikingly, this cooperation resulted in the development of a spontaneous and severe form of EAE characterized by the specific presence of inflammatory foci in the spinal cords and optic nerves of the animals. This lesion distribution pattern is very similar to that of human NMO.

B lymphocytes have been implicated in several autoimmune diseases, mostly because of their capacity to produce specific autoantibodies. B cells and plasma cells are often present in MS lesions (30,

31), and oligoclonal Ig bands have been observed in the cerebrospinal fluid of many but not all MS patients (32, 33). The presence of Ig and products of complement activation cascade deposited around the vessels suggests a pathogenic role for autoantibodies in NMO (8). In addition, a serum IgG autoantibody (NMO-IgG) serves as a specific marker for NMO (34). Recent work has shown that the NMO-IgG is not specific for myelin antigens but selectively binds to the aquaporin-4 water channel, a component of the dystroglycan protein complex located in astrocytic foot processes at the blood-brain barrier (35).

The high expression of class II MHC and costimulatory molecules by activated B cells suggest that they could also play a role in driving the T cell responses as a result of antigen presentation to large numbers of antigen-specific T cells (36, 37). In vivo, depletion of B cells from normal mice can reduce the magnitude of the immune response, suggesting that B cells contribute to the T cell response (38–41), although primary T cell responses can also develop in B cell–deficient mice (42). Therefore, a number of reports suggested that antigen-specific B cells induce naive CD4+ T cell proliferation in vivo (43–45). The importance of B cells as APCs in some autoimmune diseases such as proteoglycan-induced autoimmune arthritis has recently been demonstrated (46). In contrast with this arthritis model, EAE is generally considered to be mainly T cell driven (28). Nevertheless, it is important to note that B lymphocytes are required for the induction of EAE when MOG protein, but not MOG peptide, is used for the induction of EAE (19). Using a double antigen-specific transgenic model, we demonstrate here that, in contrast to wild-type splenocytes containing the classical APCs, MOG-specific B cells were able to stimulate the proliferation of MOG-specific T cells in the presence of a limited amount of rMOG. Since IgH^MOG B cells only recognize conformationally dependent epitopes of MOG but not MOG aa 35–55 (47), the enhanced T cell response in the presence of IgH^MOG B cells and MOG most likely resulted from the capture of MOG through B cell surface Ig that caused enhanced presentation of the antigen rather than direct presentation of MOG aa 35–55 epitope.

Ex vivo analysis of T cells from TCR^MOG×IgH^MOG mice revealed that unless mice exhibited clinical disease, there was no marked increase in the number of activated T cells in the periphery (Figure 4). Development of Devic-like disease correlated with the infiltration of both T and B cells into the spinal cord (Figure 3B and Figure 5A). The disease was also associated with the presence of lymphoid follicle–like structures in the spinal cords of TCR^MOG×IgH^MOG mice with Devic-like disease, suggesting an active cooperation between T and B cells in situ (Figure 3C). Similar to actively induced EAE, we observed that both IL-17– and IFN-γ–producing T cells infiltrated the CNS of TCR^MOG×IgH^MOG mice with Devic-like disease. Because of the low frequency of spontaneous disease observed in the TCR^MOG mice, it was not possible to perform parallel intracellular cytokine staining of CD4+ T cells infiltrating the brains of TCR^MOG mice with spontaneous EAE. However, IL-17 mRNA expression was greater in the spinal cords of TCR^MOG×IgH^MOG mice with Devic-like disease than in TCR^MOG mice with EAE. Therefore the increase in IL-17 expression in the CNS of TCR^MOG×IgH^MOG mice with Devic-like disease might reflect an increase in the number of pathogenic Th-17 cells. Alternatively, we cannot exclude the possibility that other cell types might be responsible for the enhanced IL-17 production. The role of the CNS cytokine milieu and MOG-specific B cells in the differentiation of Th-17 cells is currently under investigation.

Th cells are important for the differentiation of B cells into Ig-secreting plasma cells or long-lived memory B cells. In addition, interaction between antigen-specific T and B cells is required for B cell maturation and Ig isotype class switching. Consistent with the role played by Th cells in the maturation of B cells, we also observed that B cells from TCR^{MOG}×IgH^{MOG} mice underwent class switching from IgM to IgG1 in vivo. Ig switch is dependent on the subset of T cells providing help to B cells, and IgG1 is regarded as a Th2-dependent isotype (48). In TCR^{MOG}×IgH^{MOG} mice, however, the T cell response seems to be biased toward Th1 cells, since we only detected IFN-γ and not Th2 cytokines in cultures of TCR^{MOG} or TCR^{MOG}×IgH^{MOG} mouse spleen cells. In addition, we observed an increase in the number of B7.1-expressing B cells in TCR^{MOG}×IgH^{MOG} mice with Devic-like disease. B7.1 is a costimulatory molecule associated with enhanced Th1 responses. Therefore, the requirement for Th2 responses in IgG1 class switching might not be absolute in this model. In support of this hypothesis are previously published results showing that mice deficient in the Th2-specific cytokine IL-4 have diminished but still robust production of IgG1 (48). Alternatively, other factors present in the microenvironment might contribute to the IgG1 class switching observed in TCR^{MOG}×IgH^{MOG} mice. Taken together, the TCR^{MOG}×IgH^{MOG} model provides an interesting and, to the best of our knowledge, unique model to study the induction and cooperation of effector autopathogenic T and B cell responses in vivo and in autoimmunity.

In TCR^{MOG}×IgH^{MOG} mice it is unlikely that MOG-specific antibodies themselves are responsible for the initiation of spontaneous Devic-like disease, since we did not observe a substantial difference in the level of MOG-specific antibodies between healthy and diseased TCR^{MOG}×IgH^{MOG} mice (Figure 4C), and the transfer of serum from TCR^{MOG}×IgH^{MOG} mice to TCR^{MOG} mice did not induce EAE or Devic-like disease (data not shown). However, the combination of enhanced antibody production and a robust MOG-specific pathogenic T cell response might be responsible for the fulminant disease observed in TCR^{MOG}×IgH^{MOG} mice. In addition, the antibody and T lymphocyte specificity might play a role in determining the specific lesion distribution pattern as follows: First, the amount of antigen might be important. Previously we reported that there is relatively more MOG expressed in the optic nerves than in the spinal cords of C57BL/6 mice (23). Here we additionally demonstrated that mRNA for MOG was more abundant in the spinal cords than the brains of these mice. It is therefore possible that a differential expression of MOG protein results in predominant attack of optic nerves and spinal cords in TCR^{MOG}×IgH^{MOG} mice because there are relatively higher levels of the target antigen. Second, the accessibility of the autoantigen might be a critical factor. While the white matter in the spinal cord is on the outside and bathed in the cerebrospinal fluid, the gray matter is on the outside in the cerebellum and cerebrum. In the TCR^{MOG}×IgH^{MOG} mice, the inflammatory infiltrates in the subarachnoid space surrounding the spinal cord and around the optic nerves were more numerous than generally observed in induced EAE models and TCR^{MOG} mice with spontaneous EAE. Therefore, because MOG antigen might be more accessible in the spinal cords and optic nerves, enhanced MOG-specific T and B cell responses generated in TCR^{MOG}×IgH^{MOG} mice might preferentially attack these CNS areas, resulting in selective lesion distribution similar to that of NMO.

Autoimmune diseases have a complex pathogenesis, and the TCR transgenic mice have proven to be valuable tools to investigate the behavior of self-reactive T cells, their interactions with their anti-genic targets, and their induction of disease. Several TCR transgenic mice specific for autoantigens have been generated, and many of the autoantigen epitopes recognized by transgenic T cells have restricted expression in the CNS (49). Despite the striking increase in the frequency of self-reactive T cells in most of the TCR transgenic mouse lines, however, it is noteworthy that spontaneous autoimmune diseases do not occur in 100% of the animals. For example, 60% of PLP TCR transgenic mice develop spontaneous EAE (50), and the incidence of spontaneous EAE in MBP aa 1–11–specific TCR transgenic mice ranges from 0% to 14% depending on the line (51, 52). While 47% of TCR^{MOG} mice develop spontaneous clinical optic neuritis, only 4% of these animals develop spontaneous EAE (23). The initiation of disease most likely requires adequate priming of the auto-immune response and/or control of regulatory T cell responses. In one of the MBP-specific TCR transgenic lines, spontaneous disease occurs in 15% of the animals housed in a pathogen-free facility and 43% of those housed in conventional facilities (51), suggesting a role for infectious agents as triggers of the disease. At the present time, the environmental factor(s) in specific pathogen–free facilities that may initiate spontaneous EAE and are responsible for differences in incidence of spontaneous EAE remain unidentified. Moreover, the mechanisms underlying initiation of spontaneous EAE by infectious agents remain to be elucidated. The inflammatory response generated by infection could trigger the autoreactive T cell response and initiate autoimmune diseases. Alternatively, molecular mimicry between microbial and self antigens has been proposed as a mechanism for the development of EAE (53). Of particular relevance in this regard to the present study is the fact that there are a large number of molecular homologs of the extracellular domain of MOG. Specifically, the butyrophilin gene products exhibit linear aa sequence homologies with MOG ranging from 35% to 50% and have in some cases been shown to exhibit molecular mimicry with MOG (54). In TCR^{MOG}×IgH^{MOG} mice, autoreactive MOG-specific T cells may recognize an antigen mimicking MOG that is present in the peripheral immune compartment and then get further activated and amplified by MOG presented by large numbers of MOG-specific B cells. This might then lead to a high frequency of spontaneous disease. Since the restricted expression of MOG to the CNS has recently been challenged (55), it is also possible that MOG itself expressed in the periphery or released into the peripheral circulation could be presented to autoreactive T cells by MOG-specific B cells very efficiently. Alternatively, the increased incidence of spontaneous EAE observed in MBP TCR transgenic mice crossed to RAG-deficient mice and therefore lacking regulatory T cells expressing endogenous TCR shows the importance of regulatory cells in keeping autoreactive T cells in check (49). Since only 4% of TCR^{MOG} mice and 60% of TCR^{MOG}×IgH^{MOG} mice develop spontaneous EAE (23), we compared the number of regulatory cells between these 2 strains. Although we found that the number of CD4$^+$Foxp3$^+$ T cells was low in TCR^{MOG} mice (around 2%), it was similar in TCR^{MOG}×IgH^{MOG} mice. Additional experiments are necessary to determine whether B cells can modulate the activity of regulatory cells.

In summary, TCR^{MOG}×IgH^{MOG} mice represent a useful model to determine the factors responsible for different lesion localization and to study the role of T cell/B cell cooperation in the induction of autoimmune pathologies. In addition, since TCR^{MOG}×IgH^{MOG} mice develop a high incidence of spontaneous disease involving both T and B cells, these mice may be useful for testing the biology of T cell/B cell cooperation in the genesis of autoimmune diseases and for testing novel therapies for MS and Devic disease.

Methods

Animals. C57BL/6 mice transgenic for a TCR with specificity for the peptide MOG aa 35–55 (TCR[MOG] mice; also referred to as 2D2 mice) were extensively described previously (23). As control for TCR[MOG] mice, we used TCR[OVA] mice (also referred to as OT-II mice), which are transgenic for a TCR recognizing the peptide OVA aa 323–339 (The Jackson Laboratory).

IgH[MOG] mice (also referred to as Th mice), which contain MOG-specific B cells, were generated by replacing the germline *JH* locus with the rearranged Ig heavy-chain (IgH) variable (*V*) gene of a pathogenic MOG-specific monoclonal antibody (24). The B cells exclusively express the transgenic H chains, and one-third bind MOG. As control for the IgH[MOG] mice, we used NP-specific IgH[NP] mice (also referred to as B1.8 mice; ref. 56).

Mice were housed in a specific pathogen–free, viral antibody–free animal facility at the Harvard Institutes of Medicine. All breeding and experiments were reviewed and approved by the Institutional Animal Care and Use Committee of Harvard Medical School. Serums from 4- to 10-week-old mice were obtained at sacrifice by cardiac puncture.

Antigens. MOG aa 35–55 peptide (MEVGWYRSPFSRVVHLYRNGK) and OVA aa 323–336 peptide (ISQAVHAAHAEINE) were obtained from the Biopolymer Facility, Center for Neurological Diseases, Brigham and Women's Hospital. A plasmid construct encoding the extracellular domain of rat MOG protein (MOG aa 1–125) was generously provided by C. Linington (University of Aberdeen, Aberdeen, United Kingdom), and rMOG protein was purified from inclusion bodies (57). OVA was purchased from Sigma-Aldrich.

Cell isolation. T and B lymphocytes were isolated from spleens and lymph nodes using anti-CD4 and anti-B220 columns, respectively, according to the manufacturer's instructions (Miltenyi Biotec). Purity of the positively selected cell populations was >95% as assessed by flow cytometry. For the analysis of B cell proliferation and activation in the presence of antigen-specific T cells, we used T cell lines obtained by 2 rounds of stimulation of lymphocytes from TCR transgenic mice with 10 μg/ml MOG aa 35–55 or OVA aa 323–326 in the presence of irradiated splenocytes and 20 U/ml IL-2.

Proliferation assays. Cells were grown in RPMI supplemented with 10% FCS, β-mercaptoethanol, L-glutamine, gentamicin sulfate, and penicillin/streptomycin. For thymidine proliferation assay, either 5×10^6 cells/ml total splenocytes or 2.5×10^5 cells/ml purified CD4^{+} cells plus 2.5×10^6 cells/ml purified B220^{+} B cells were cultured for 72 hours in 96-well plates in the presence of different concentrations of the rMOG protein or MOG aa 35–55 peptide (range, 0.01–100 μg/ml). Cells were pulsed with 1 μCi ^{3}H-thymidine for the last 16 hours of incubation. Mean thymidine incorporation in triplicate wells was measured using a β counter (LS 5000; Beckman Coulter).

For the assessment of proliferation by CFSE dilution assay, the cells were labeled with CFSE (Invitrogen) at 2 μM in PBS, washed, and cultured at 5×10^5 cells/ml for 2–4 days according to the specific stimulation protocol. Cells were then harvested and analyzed by flow cytometry.

Flow cytometry. Unlabeled or CFSE-labeled cells were blocked with antibodies to the FcγIII/II receptors (CD16/CD32) to avoid nonspecific staining and were subsequently labeled at 4°C with the following monoclonal antibodies (BD Biosciences): anti-CD23–PE, anti-CD40L–PE, anti-CD69–PE, anti-CD80–PE, anti-CD86–PE, anti-IgM–PE, anti-IgG1–PE, anti-IgG2a–PE, anti-IgG2b–PE, anti-IgG3–PE, anti-CD4–allophycocyanin, and anti-B220–allophycocyanin. Isotype- and concentration-matched control antibodies were used to assess nonspecific staining. Cells were then fixed in 0.3% paraformaldehyde and kept at 4°C until analysis.

For the detection of intracellular cytokines, the cells were restimulated for 5 hours with PMA (50 ng/ml) and ionomycin (1 μM), in the presence of 3 μM monencin for the last 3 hours. The cells were then stained for surface markers and fixed. Subsequently, the cells were permeabilized with saponin and stained with PE-labeled anti-cytokine antibodies resuspended in saponin buffer.

The cells were analyzed on a 4-color FACSort (BD Biosciences), and lymphocytes were gated on forward and side scatter as well as on CD4 and B220 for T and B cells, respectively.

ELISA. IL-2, IL-4, IL-10, and IFN-γ concentrations were determined in cell culture supernatant by a standard sandwich ELISA by coating 96-well plates with the appropriate anti-cytokine monoclonal antibodies (BD Biosciences), incubating the plates with the culture supernatant overnight, and detecting the bound cytokines with a second biotinylated anti-cytokine antibody and avidin peroxidase. Results were reported in pg/ml according to a standard dilution curve.

For measuring MOG-specific antibodies in serum, 96-well plates were coated with 4 μg/ml MOG in PBS, blocked, and incubated with sera (1:40 and 1:200 dilution for IgM and 1:200 and 1:1,000 dilution for IgG isotypes) for 2 hours. After washing, the serum antibodies retained by the plate-bound MOG were detected by biotinylated, isotype-specific anti-Ig antibodies (BD Biosciences) and avidin peroxidase. Nonspecific binding was assessed using OVA-coated plates as negative control. Results were reported as OD.

EAE assessment. Clinical assessment of EAE was performed daily, and mice were scored for disease according to the following criteria: 0, no disease; 1, decreased tail tone; 2, hind-limb weakness or partial paralysis; 3, complete hind-limb paralysis; 4, front- and hind-limb paralysis; 5, moribund state.

Histology. Animals were sacrificed after 3 months of observation for development of clinical signs of EAE or after at least 2 weeks of EAE. Brains, spinal cords, and optic nerves were removed and fixed in 10% formalin. Paraffin-embedded sections were stained with hematoxylin and eosin, Luxol fast blue, and reticulin and by Bielschowsky preparation for light microscopy. Immunohistochemistry was performed on cryosections using antibodies to CD4, TCR Vβ11, and B220.

Statistics. Ig serum levels in TCR[MOG]×IgH[MOG] mice versus TCR[MOG] or IgH[MOG] control mice were compared by 2-tailed Student's *t* test. *P* values less than 0.05 were considered to be statistically significant.

Address correspondence to: Vijay K. Kuchroo, Center for Neurologic Diseases, HIM780, Brigham and Women's Hospital and Harvard Medical School, 77 Avenue Louis Pasteur, Boston, Massachusetts 02115, USA. Phone: (617) 525-5350; Fax: (617) 525-5566; E-mail: vkuchroo@rics.bwh.harvard.edu.

Estelle Bettelli and Dominique Baeten contributed equally to this work.

1. Lassmann, H. 1998. Pathology of multiple sclerosis. In *McAlpine's multiple sclerosis*. A. Compston, et al., editors. Churchill Livingstone. Hong Kong, People's Republic of China. 323–358.

2. Ghezzi, A., et al. 1999. Long-term follow-up of isolated optic neuritis: the risk of developing multiple sclerosis, its outcome, and the prognostic role of paraclinical tests. *J. Neurol.* **246**:770–775.

3. Soderstrom, M. 2001. Optic neuritis and multiple sclerosis. *Acta Ophthalmol. Scand.* **79**:223–227.

4. Misu, T., et al. 2002. Pure optic-spinal form of multiple sclerosis in Japan. *Brain.* **125**:2460–2468.

5. Wingerchuk, D.M., and Weinshenker, B.G. 2003. Neuromyelitis optica: clinical predictors of a relapsing course and survival. *Neurology.* **60**:848–853.

6. Wingerchuk, D.M., Hogancamp, W.F., O'Brien, P.C., and Weinshenker, B.G. 1999. The clinical course of neuromyelitis optica (Devic's syndrome). *Neurology.* **53**:1107–1114.

7. Cree, B.A., Goodin, D.S., and Hauser, S.L. 2002. Neuromyelitis optica. *Semin. Neurol.* **22**:105–122.

8. Lucchinetti, C.F., et al. 2002. A role for humoral mechanisms in the pathogenesis of Devic's neuromyelitis optica. *Brain.* **125**:1450–1461.

9. Keegan, M., et al. 2002. Plasma exchange for severe attacks of CNS demyelination: predictors of response. *Neurology.* **58**:143–146.

10. Zamvil, S.S., et al. 1986. T-cell epitope of the autoantigen myelin basic protein that induces encephalomyelitis. *Nature.* **324**:258–260.

11. Sobel, R.A., Greer, J.M., and Kuchroo, V.K. 1994. Minireview: autoimmune responses to myelin proteolipid protein. *Neurochem. Res.* **19**:915–921.

12. Mendel, I., Kerlero de Rosbo, N., and Ben-Nun, A. 1995. A myelin oligodendrocyte glycoprotein peptide induces typical chronic experimental autoimmune encephalomyelitis in H-2b mice: fine specificity and T cell receptor V beta expression of encephalitogenic T cells. *Eur. J. Immunol.* **25**:1951–1959.

13. Baron, J.L., Madri, J.A., Ruddle, N.H., Hashim, G., and Janeway, C.A., Jr. 1993. Surface expression of alpha 4 integrin by CD4 T cells is required for their entry into brain parenchyma. *J. Exp. Med.* **177**:57–68.

14. Kuchroo, V.K., et al. 1993. Cytokines and adhesion molecules contribute to the ability of myelin proteolipid protein-specific T cell clones to mediate experimental allergic encephalomyelitis. *J. Immunol.* **151**:4371–4382.

15. Langrish, C.L., et al. 2005. IL-23 drives a pathogenic T cell population that induces autoimmune inflammation. *J. Exp. Med.* **201**:233–240.

16. Park, H., et al. 2005. A distinct lineage of CD4 T cells regulates tissue inflammation by producing interleukin 17. *Nat. Immunol.* **6**:1133–1141.

17. Hjelmstrom, P., Juedes, A.E., Fjell, J., and Ruddle, N.H. 1998. B-cell-deficient mice develop experimental allergic encephalomyelitis with demyelination after myelin oligodendrocyte glycoprotein sensitization. *J. Immunol.* **161**:4480–4483.

18. Svensson, L., et al. 2002. A comparative analysis of B cell-mediated myelin oligodendrocyte glycoprotein-experimental autoimmune encephalomyelitis pathogenesis in B cell-deficient mice reveals an effect on demyelination. *Eur. J. Immunol.* **32**:1939–1946.

19. Lyons, J.A., San, M., Happ, M.P., and Cross, A.H. 1999. B cells are critical to induction of experimental allergic encephalomyelitis by protein but not by a short encephalitogenic peptide. *Eur. J. Immunol.* **29**:3432–3439.

20. Oliver, A.R., Lyon, G.M., and Ruddle, N.H. 2003. Rat and human myelin oligodendrocyte glycoproteins induce experimental autoimmune encephalomyelitis by different mechanisms in C57BL/6 mice. *J. Immunol.* **171**:462–468.

21. Lyons, J.A., Ramsbottom, M.J., and Cross, A.H. 2002. Critical role of antigen-specific antibody in experimental autoimmune encephalomyelitis induced by recombinant myelin oligodendrocyte glycoprotein. *Eur. J. Immunol.* **32**:1905–1913.

22. Fillatreau, S., Sweenie, C.H., McGeachy, M.J., Gray, D., and Anderton, S.M. 2002. B cells regulate autoimmunity by provision of IL-10. *Nat. Immunol.* **3**:944–950.

23. Bettelli, E., et al. 2003. Myelin oligodendrocyte glycoprotein-specific T cell receptor transgenic mice develop spontaneous autoimmune optic neuritis. *J. Exp. Med.* **197**:1073–1081.

24. Litzenburger, T., et al. 1998. B lymphocytes producing demyelinating autoantibodies: development and function in gene-targeted transgenic mice. *J. Exp. Med.* **188**:169–180.

25. Slavin, A.J., et al. 2001. Requirement for endocytic antigen processing and influence of invariant chain and H-2M deficiencies in CNS autoimmunity. *J. Clin. Invest.* **108**:1133–1139. doi:10.1172/JCI200113360.

26. Serafini, B., Rosicarelli, B., Magliozzi, R., Stigliano, E., and Aloisi, F. 2004. Detection of ectopic B-cell follicles with germinal centers in the meninges of patients with secondary progressive multiple sclerosis. *Brain Pathol.* **14**:164–174.

27. Corcione, A., et al. 2005. B-cell differentiation in the CNS of patients with multiple sclerosis. *Autoimmun. Rev.* **4**:549–554.

28. Kuchroo, V.K., et al. 2002. T cell response in experimental autoimmune encephalomyelitis (EAE): role of self and cross-reactive antigens in shaping, tuning, and regulating the autopathogenic T cell repertoire. *Annu. Rev. Immunol.* **20**:101–123.

29. Bettelli, E., et al. 2006. Reciprocal developmental pathways for the generation of pathogenic effector T(H)17 and regulatory T cells. *Nature.* **441**:235–238.

30. Esiri, M.M. 1980. Multiple sclerosis: a quantitative and qualitative study of immunoglobulin-containing cells in the central nervous system. *Neuropathol. Appl. Neurobiol.* **6**:9–21.

31. Baranzini, S.E., et al. 1999. B cell repertoire diversity and clonal expansion in multiple sclerosis brain lesions. *J. Immunol.* **163**:5133–5144.

32. Qin, Y., et al. 2003. Intrathecal B-cell clonal expansion, an early sign of humoral immunity, in the cerebrospinal fluid of patients with clinically isolated syndrome suggestive of multiple sclerosis. *Lab. Invest.* **83**:1081–1088.

33. Owens, G.P., et al. 2003. Single-cell repertoire analysis demonstrates that clonal expansion is a prominent feature of the B cell response in multiple sclerosis cerebrospinal fluid. *J. Immunol.* **171**:2725–2733.

34. Lennon, V.A., et al. 2004. A serum autoantibody marker of neuromyelitis optica: distinction from multiple sclerosis. *Lancet.* **364**:2106–2112.

35. Lennon, V.A., Kryzer, T.J., Pittock, S.J., Verkman, A.S., and Hinson, S.R. 2005. IgG marker of optic-spinal multiple sclerosis binds to the aquaporin-4 water channel. *J. Exp. Med.* **202**:473–477.

36. Lanzavecchia, A. 1985. Antigen-specific interaction between T and B cells. *Nature.* **314**:537–539.

37. Bryant, P., and Ploegh, H. 2004. Class II MHC peptide loading by the professionals. *Curr. Opin. Immunol.* **16**:96–102.

38. Hayglass, K.T., Naides, S.J., Scott, C.F., Jr., Benacerraf, B., and Sy, M.S. 1986. T cell development in B cell-deficient mice. IV. The role of B cells as antigen-presenting cells in vivo. *J. Immunol.* **136**:823–829.

39. Ron, Y., and Sprent, J. 1987. T cell priming in vivo: a major role for B cells in presenting antigen to T cells in lymph nodes. *J. Immunol.* **138**:2848–2856.

40. Janeway, C.A., Jr., Ron, J., and Katz, M.E. 1987. The B cell is the initiating antigen-presenting cell in peripheral lymph nodes. *J. Immunol.* **138**:1051–1055.

41. Kurt-Jones, E.A., et al. 1988. The role of antigen-presenting B cells in T cell priming in vivo. Studies of B cell-deficient mice. *J. Immunol.* **140**:3773–3778.

42. Epstein, M.M., Di Rosa, F., Jankovic, D., Sher, A., and Matzinger, P. 1995. Successful T cell priming in B cell-deficient mice. *J. Exp. Med.* **182**:915–922.

43. Townsend, S.E., and Goodnow, C.C. 1998. Abortive proliferation of rare T cells induced by direct or indirect antigen presentation by rare B cells in vivo. *J. Exp. Med.* **187**:1611–1621.

44. Garside, P., et al. 1998. Visualization of specific B and T lymphocyte interactions in the lymph node. *Science.* **281**:96–99.

45. MacLennan, I.C., et al. 1997. The changing preference of T and B cells for partners as T-dependent antibody responses develop. *Immunol. Rev.* **156**:53–66.

46. O'Neill, S.K., et al. 2005. Antigen-specific B cells are required as APCs and autoantibody-producing cells for induction of severe autoimmune arthritis. *J. Immunol.* **174**:3781–3788.

47. Breithaupt, C., et al. 2003. Structural insights into the antigenicity of myelin oligodendrocyte glycoprotein. *Proc. Natl. Acad. Sci. U. S. A.* **100**:9446–9451.

48. Kuhn, R., Rajewsky, K., and Muller, W. 1991. Generation and analysis of interleukin-4 deficient mice. *Science.* **254**:707–710.

49. Lafaille, J.J. 2004. T-cell receptor transgenic mice in the study of autoimmune diseases. *J. Autoimmun.* **22**:95–106.

50. Waldner, H., Whitters, M.J., Sobel, R.A., Collins, M., and Kuchroo, V.K. 2000. Fulminant spontaneous autoimmunity of the central nervous system in mice transgenic for the myelin proteolipid protein-specific T cell receptor. *Proc. Natl. Acad. Sci. U. S. A.* **97**:3412–3417.

51. Goverman, J., et al. 1993. Transgenic mice that express a myelin basic protein-specific T cell receptor develop spontaneous autoimmunity. *Cell.* **72**:551–560.

52. Lafaille, J.J., Nagashima, K., Katsuki, M., and Tonegawa, S. 1994. High incidence of spontaneous autoimmune encephalomyelitis in immunodeficient anti-myelin basic protein T cell receptor transgenic mice. *Cell.* **78**:399–408.

53. Oldstone, M.B. 1987. Molecular mimicry and autoimmune disease. *Cell.* **50**:819–820.

54. Stefferl, A., et al. 2000. Butyrophilin, a milk protein, modulates the encephalitogenic T cell response to myelin oligodendrocyte glycoprotein in experimental autoimmune encephalomyelitis. *J. Immunol.* **165**:2859–2865.

55. Pagany, M., et al. 2003. Myelin oligodendrocyte glycoprotein is expressed in the peripheral nervous system of rodents and primates. *Neurosci. Lett.* **350**:165–168.

56. Sonoda, E., et al. 1997. B cell development under the condition of allelic inclusion. *Immunity.* **6**:225–233.

57. Adelmann, M., et al. 1995. The N-terminal domain of the myelin oligodendrocyte glycoprotein (MOG) induces acute demyelinating experimental autoimmune encephalomyelitis in the Lewis rat. *J. Neuroimmunol.* **63**:17–27.